

**Zeitschrift:** IABSE congress report = Rapport du congrès AIPC = IVBH  
Kongressbericht

**Band:** 8 (1968)

**Artikel:** A model for the study of soil-structure interaction

**Autor:** Agabein, M.E. / Parmelee, R.A. / Lee, S.L.

**DOI:** <https://doi.org/10.5169/seals-8867>

### **Nutzungsbedingungen**

Die ETH-Bibliothek ist die Anbieterin der digitalisierten Zeitschriften. Sie besitzt keine Urheberrechte an den Zeitschriften und ist nicht verantwortlich für deren Inhalte. Die Rechte liegen in der Regel bei den Herausgebern beziehungsweise den externen Rechteinhabern. [Siehe Rechtliche Hinweise.](#)

### **Conditions d'utilisation**

L'ETH Library est le fournisseur des revues numérisées. Elle ne détient aucun droit d'auteur sur les revues et n'est pas responsable de leur contenu. En règle générale, les droits sont détenus par les éditeurs ou les détenteurs de droits externes. [Voir Informations légales.](#)

### **Terms of use**

The ETH Library is the provider of the digitised journals. It does not own any copyrights to the journals and is not responsible for their content. The rights usually lie with the publishers or the external rights holders. [See Legal notice.](#)

**Download PDF:** 02.02.2025

**ETH-Bibliothek Zürich, E-Periodica, <https://www.e-periodica.ch>**



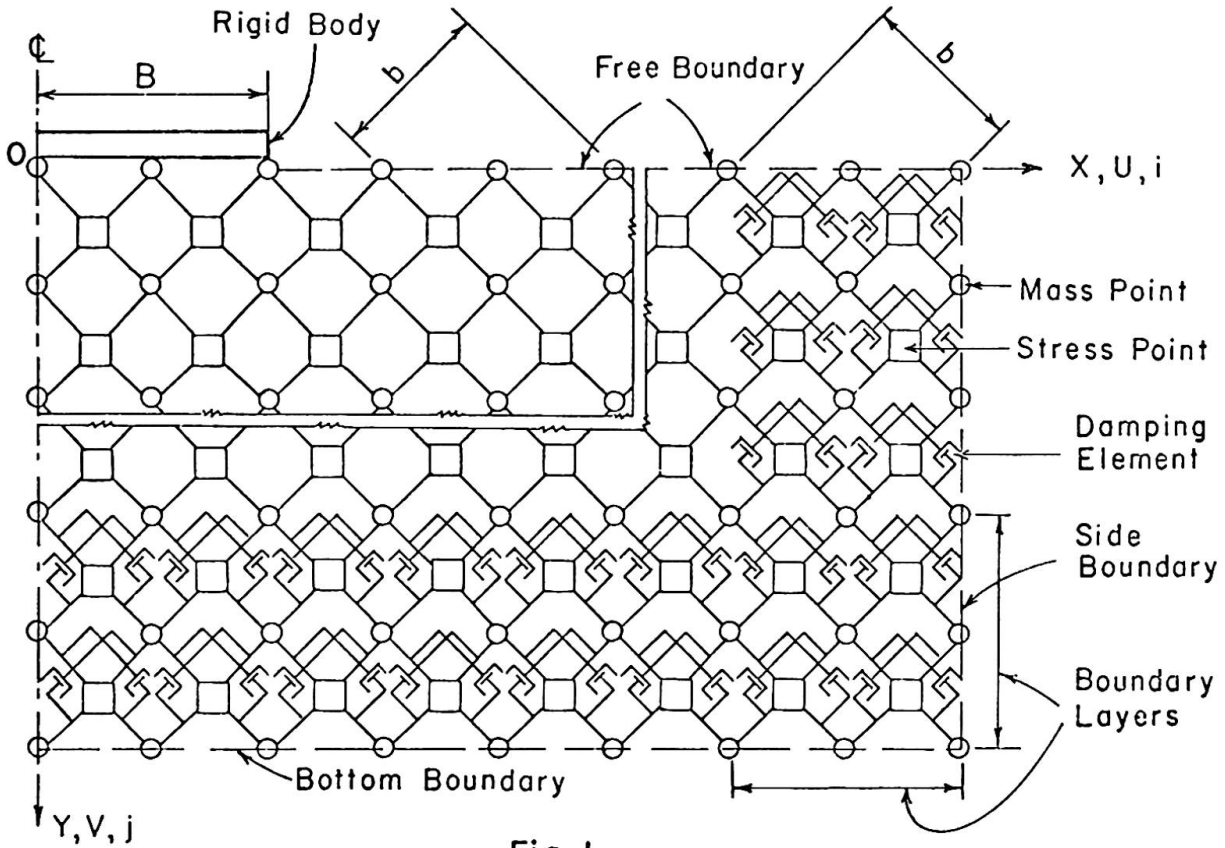


Fig. 1

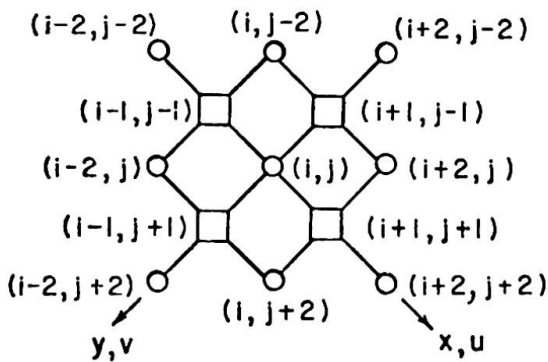


Fig. 2

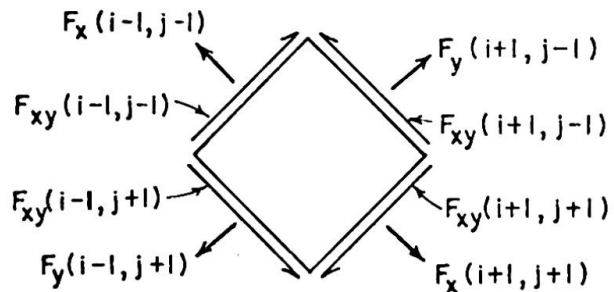


Fig. 3

2. Formulation of the Model

The lumped-parameter model for plane strain problems introduced by Ang and Harper [ 9 ] is used to represent the foundation medium which is assumed to be elastic, homogeneous and isotropic. The model consists essentially of mass points and stress points arranged as shown in Fig. 1, where the boundaries of the model and the reference coordinates, X- and Y-axes, are indicated.

A typical interior mass point shown in Fig. 2 contains the mass  $m = \rho b^2/2$  of the foundation medium, where  $b$  is the mesh size of the model in the x- and y-axes and  $\rho$  is the mass density of the medium. The displacement, velocities and accelerations are defined at the mass points. The average stresses and

strains are defined at the stress points, which are assumed to be in a state of homogeneous stress and strain. The strains at a stress point are determined from the displacements of adjacent mass points, and the forces acting on a mass point are calculated from the stresses at adjacent stress points (Fig. 3).

For small deformation and plane strain conditions, the strain-displacement relationships for a typical interior stress point (i+1,j+1), as shown in Fig. 2, take the form

$$\begin{aligned} \epsilon_x (i+1, j+1) &= \frac{u(i+2, j+2) - u(i, j)}{b} \\ \epsilon_y (i+1, j+1) &= \frac{v(i, j+2) - v(i+2, j)}{b} \\ \epsilon_{xy} (i+1, j+1) &= \frac{1}{2b} [u(i, j+2) - u(i+2, j) + v(i+2, j+2) - v(i, j)] \end{aligned} \tag{1}$$

In these equations,  $\epsilon_x$ ,  $\epsilon_y$  and  $\epsilon_{xy}$  denote the strain components and u and v the displacements along the  $x^y$  and  $y^{xy}$  axes respectively.

The forces acting on an interior mass point (i,j) are shown in Fig. 3. The normal forces  $F_x$  and  $F_y$  and the shearing force  $F_{xy}$  exerted by the adjacent stress points are equal to the products of the corresponding average stresses and the effective area on which they act and are given by

$$\begin{aligned} F_x (i+1, j+1) &= \frac{b}{2} \sigma_x (i+1, j+1) \\ F_y (i+1, j+1) &= \frac{b}{2} \sigma_y (i+1, j+1) \\ F_{xy} (i+1, j+1) &= \frac{b}{2} \sigma_{xy} (i+1, j+1) \end{aligned} \tag{2}$$

in which  $\sigma_x$ ,  $\sigma_y$  and  $\sigma_{xy}$  are the normal and shearing stresses along the x- and y-axes.

From Fig. 3, the equations of motion for a typical interior mass point (i,j) along the x and y directions are, in view of (2),

$$\begin{aligned} \frac{\sigma_x (i+1, j+1) - \sigma_x (i-1, j-1)}{b} + \frac{\sigma_{xy} (i-1, j+1) - \sigma_{xy} (i+1, j-1)}{b} &= \rho \ddot{u}(i, j) \\ \frac{\sigma_y (i-j, j+1) - \sigma_y (i+1, j-1)}{b} + \frac{\sigma_{xy} (i+1, j+1) - \sigma_{xy} (i-1, j-1)}{b} &= \rho \ddot{v}(i, j) \end{aligned} \tag{3}$$

Applying Hooke's law to (3) and substituting for the strains from (1), the resulting equations of motion of a typical interior mass point in terms of the displacements are

$$\begin{aligned} &\frac{G}{b^2} [u(i+2, j+2) + u(i-2, j+2) - 4u(i, j) + u(i-2, j-2) + u(i+2, j-2)] \\ + \frac{\lambda+G}{b^2} [u(i+2, j+2) - 2u(i, j) + u(i-2, j-2) - v(i-2, j) + v(i, j-2) \\ &\quad - v(i+2, j) + v(i, j+2)] = \rho \ddot{u}(i, j) \\ &\frac{G}{b^2} [v(i-2, j+2) + v(i-2, j-2) - 4v(i, j) + v(i+2, j-2) + v(i+2, j+2)] + \end{aligned} \tag{4}$$

$$\begin{aligned}
& + \frac{\lambda+G}{b^2} \left[ v(i-2, j+2) - 2v(i, j) + v(i+2, j-2) + u(i, j+2) - u(i-2, j) \right. \\
& \quad \left. + u(i, j-2) - u(i+2, j) \right] = \rho \ddot{v}(i, j) \quad (4)
\end{aligned}$$

in which  $\lambda = 2\nu G/(1-2\nu)$ ,  $G$  is the shear modulus and  $\nu$  the Poisson's ratio.

It is interesting to note that (1) and (4) are the central finite difference analogue of the corresponding differential equations for the continuum. On the free surface, applied stresses are defined at fictitious stress points adjacent to the boundary, while boundary displacements are defined at the boundary mass points.

### 3. Model Size and Damping

To develop the model, the harmonic rocking of an infinitely long rigid rectangular body on an elastic half space is considered. The rigid body is of width  $2B$  with mass  $M$  per unit length and the elastic half space is approximated by the lumped-parameter model as shown in Fig. 1. The boundary conditions are such that the vertical displacement of the five mass points in contact with the rigid body is  $\Psi X$ , where  $\Psi$  is the angle of rotation of the body, the free surface beyond the rigid body is stress free, the surface of contact between the base of the rigid body and the semi-infinite medium is smooth, and the displacements of the mass points on the side and bottom boundaries are assumed to vanish.

The equation of motion that governs the harmonic rocking of the rigid body takes the form

$$\begin{aligned}
m(5 + 16 \bar{J}) \frac{B\ddot{\Psi}}{\sqrt{2}} + G \left[ \frac{10}{\sqrt{2}} B\Psi - 2v(6,0) - 2v(6,2) - v(4,2) \right. \\
- 2v(2,2) - 2u(0,0) - 4u(2,0) + 2u(4,0) + 2u(6,0) - 2u(6,2) \\
- u(4,2) - 2u(2,2) \left. \right] + (\lambda+G) \left[ \frac{7}{\sqrt{2}} B\Psi + 2v(6,0) - 2v(4,2) \right. \\
- 3v(2,2) + u(0,0) + 2u(2,0) - u(4,0) - 2u(6,2) - 3u(4,2) \\
- u(2,2) + u(0,2) \left. \right] = 2\sqrt{2} T e^{i\omega t}/B \quad (5)
\end{aligned}$$

in which  $\bar{J} = J/\rho B^4$  is the non-dimensional inertia,  $J$  is the polar inertia of the body,  $T$  and  $\omega$  are respectively the amplitude of the applied torque and frequency of excitation, and  $t$  denotes time.

The optimum size of the model with rigid boundaries is established by varying the dimensions of the model and solving the system of equations by a high-speed digital computer for the static case, i.e.,  $\omega = 0$ . For each model size the static rotational stiffness  $T/\Psi$  is determined and compared with the analytical value [10] given by  $T/\Psi = \pi G B^2/2(1-\nu)$ . It is found that the larger the dimensions of the model, the closer is the agreement; however the computer time required becomes excessive. The model size  $X = 4B$  ( $i = 16$ ,  $b = B/\sqrt{2}$ ) and  $Y = 3.5B$  ( $j = 14$ ) yields a static stiffness with 5% accuracy and requires reasonable computational time, hence it will be used in the following study. For this model size, observing the condition of antisymmetry and the boundary conditions, the model has 104 degrees of freedom.

Next the system of equations for harmonic rocking is solved and the results obtained showed, as expected, infinitely large amplitudes at resonant frequencies. This is of course physically incorrect since in the infinite medium the

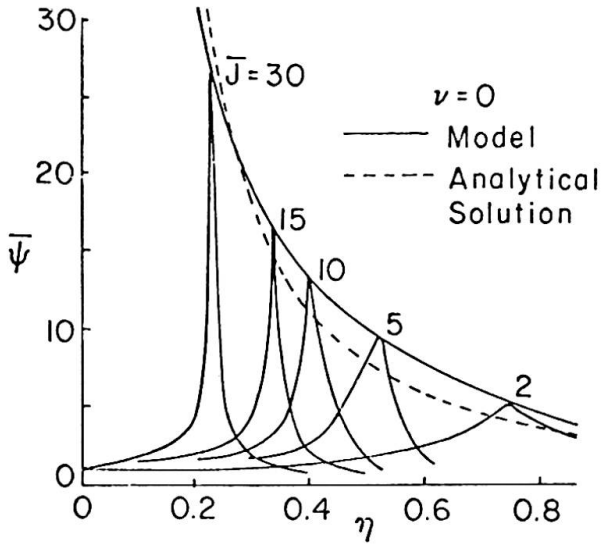


Fig. 4

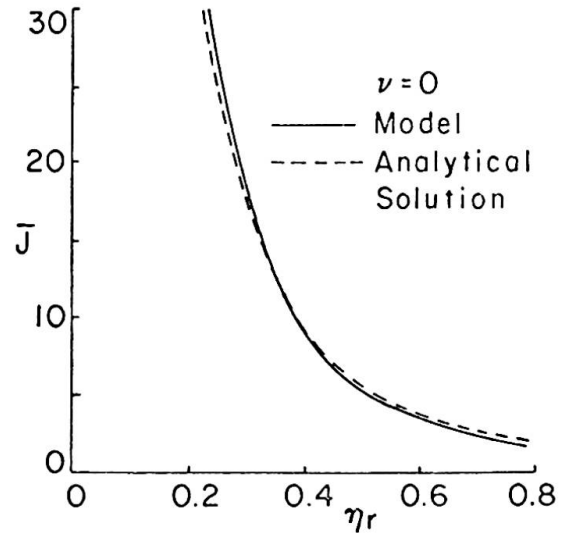


Fig. 5

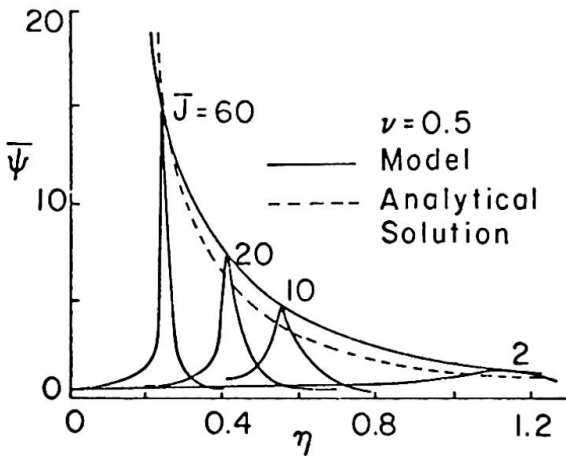


Fig. 6

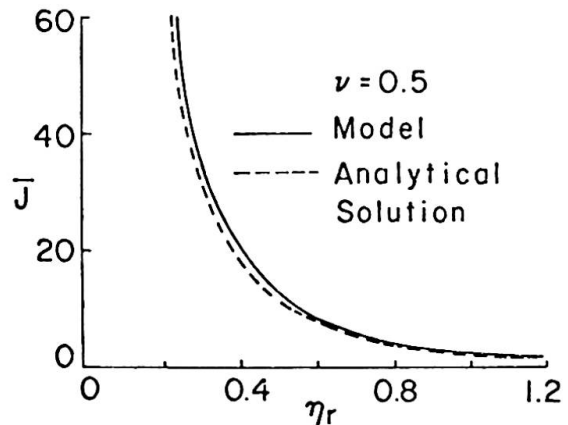


Fig. 7

energy is dissipated by the dispersion of the elastic waves far from the source of disturbance. This dissipation of energy produces a damping effect which limits the amplitudes at resonant frequencies. To build this damping effect into the finite-size model, damping elements are placed in parallel to the stress points along the two boundary layers adjacent to the side and bottom boundaries, as shown in Fig. 1. Thus the equations of motion for the boundary mass points contain damping terms which serve the purpose of dissipating the energy and reducing the reflection of waves from the boundaries. The damping coefficient  $c$  of these elements is determined by matching the amplitudes at resonant frequencies with the analytical solution [10] and depends not only on the properties of the medium and the size of the model, but also on the frequency. The value of the non-dimensional damping factor  $\bar{c} = c/\rho BV_s$ , where  $V_s = \sqrt{G/\rho}$  is the shear wave velocity, given by

$$\bar{c} = 9 - 10 \nu \tag{6}$$

is found to give reasonably good results for the frequency range of interest.

Using the values of  $\bar{c}$  defined by (6), the results for  $\nu = 0$  are shown in Figs. 4,5 and those for  $\nu = 0.5$  in Figs. 6,7. In Figs. 4,6 the non-dimensional amplitude  $\bar{\Psi} = \pi GB^2 |\Psi| / 2T$  is plotted versus the frequency factor  $\eta = B\omega/V_s$  for

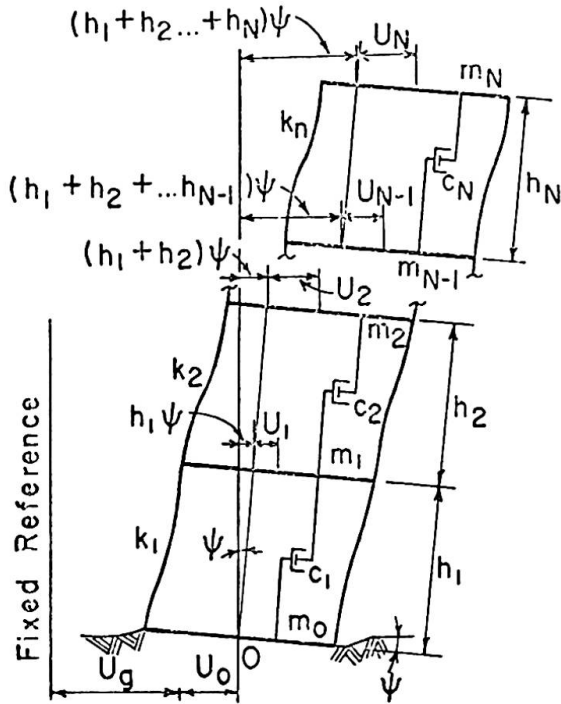


Fig. 8

4. Multiple-Story Building on Flexible Foundation

A dynamic model for an elastic N-story shear building resting on the elastic half space is shown in Fig. 8 in the deformed state. Both interaction rotation  $\Psi$  and horizontal translation  $U_0$  of the base mass  $m_0$  are allowed in contrast to rigid foundation. The interfloor damping coefficient  $c_n$ , taken as a percentage of the critical damping in the first mode of vibration of the structure supported on a rigid foundation, is assumed to be proportional to the flexural stiffness  $k_n$  of story  $n$  to eliminate the dynamic coupling between the various modes.

The soil-structure interaction system is represented by placing the building in Fig. 8 on the foundation model in Fig. 1, where the base mass of the building replaces the rigid body. No slippage is allowed in this instance. Thus the five mass points at the surface of contact undergo the same displacement as the base mass, i.e.,

$$\begin{aligned}
 V(i,0) &= \Psi X_i \\
 U(0,0) &= U(2,0) = U(4,0) = U_0
 \end{aligned}
 \tag{7}$$

In view of (7) the degree of freedom of the foundation model is 102 and that of the interaction system for  $N$  stories is  $(N + 102)$ . The  $(N + 2)$  equations of motion for the building shown in Fig. 8 are

$$\begin{aligned}
 \ddot{U}_0 \left( \frac{5}{2} \alpha + \sum_{n=0}^N \alpha_n \right) + \ddot{\Psi} \sum_{n=1}^N \alpha_n \bar{h}_n + \sum_{n=1}^N \alpha_n \ddot{U}_n + \frac{G}{\sqrt{2} m_N} \left[ \frac{10}{\sqrt{2}} U_0 - u(6,0) - u(6,2) - \right. \\
 \left. - u(4,2) - 2u(2,2) - 2u(0,2) - \frac{2}{\sqrt{2}} B\Psi - v(6,0) + v(6,2) + v(4,2) + 2v(2,2) \right]
 \end{aligned}$$

various values of the non-dimensional inertia  $\bar{J}$ . In Figs. 5,7 the non-dimensional inertia  $\bar{J}$  is plotted versus the resonant frequency factor  $\eta_r = B\omega_r/V_s$ , where  $\omega_r$  is the resonant frequency. It can be seen that the approximation of the stiffness and damping characteristics of the elastic half space by the model give, for practical purposes, results which are in satisfactory agreement with those obtained by the analytical solution [10] especially in the lower frequency range which is of primary importance in the seismic response of soil-structure interaction systems.

$$\begin{aligned}
 & + \frac{\lambda + G}{\sqrt{2} m_N} \left[ \frac{1}{\sqrt{2}} U_0 - u(6,2) + \frac{B}{\sqrt{2}} \Psi + v(6,0) - v(4,2) \right] = - \ddot{U}_g \sum_{n=0}^N \alpha_n \\
 & \ddot{U}_0 \sum_{n=1}^N \alpha_n \bar{h}_n + \ddot{\Psi} \left[ \frac{5}{4} \alpha B^2 + \frac{B^2}{3} \sum_{n=0}^N \alpha_n + \sum_{n=1}^N \alpha_n \bar{h}_n^2 \right] + \sum_{n=1}^N \alpha_n \bar{h}_n \ddot{U}_n \\
 & + \frac{GB}{\sqrt{2} m_N} \left[ \frac{5}{\sqrt{2}} B\Psi - v(6,0) - v(6,2) - \frac{1}{2} v(4,2) - v(2,2) - \frac{2}{\sqrt{2}} U_0 + u(6,0) - \right. \\
 & \left. - u(6,2) - \frac{1}{2} u(4,2) - u(2,2) \right] + \frac{(\lambda+G)B}{\sqrt{2} m_N} \left[ \frac{7}{2\sqrt{2}} B\Psi + v(6,0) - v(4,2) - \frac{3}{2} v(2,2) + \right. \\
 & \left. + \frac{1}{\sqrt{2}} U_0 - u(6,2) - \frac{3}{2} u(4,2) - \frac{1}{2} u(2,2) + \frac{1}{2} u(0,2) \right] = - \ddot{U}_g \sum_{n=1}^N \alpha_n \bar{h}_n \\
 & \alpha_n \ddot{U}_0 + \alpha_n \bar{h}_n \ddot{\Psi} + \alpha_n \ddot{U}_n - \frac{c_{n+1}}{m_N} \dot{U}_{n+1} + \frac{(c_n + c_{n+1})}{m_N} \dot{U}_n - \frac{c_n}{m_N} \dot{U}_{n-1} - \frac{k_{n+1}}{m_N} U_{n+1} + \\
 & + \frac{(k_n + k_{n+1})}{m_N} U_n - \frac{k_n}{m_N} U_{n-1} = - \ddot{U}_g \alpha_n \quad (n = 1, 2, \dots, N)
 \end{aligned}
 \tag{8}$$

in which

$$\begin{aligned}
 \alpha_n &= m_n / m_N, \quad \alpha_0 = m_0 / m_N, \quad \alpha = m / m_N, \quad \bar{h}_n = \sum_{i=1}^n h_i \\
 c_1 \dot{U}_0 &= k_1 U_0 = 0, \quad c_{N+1} = k_{N+1} = 0
 \end{aligned}
 \tag{9}$$

and  $h_n$  is the height of the  $n$ -th story,  $m_n$  the mass of the  $n$ -th floor,  $U_n$  the horizontal translation of the  $n$ -th story caused by the free field earthquake displacement  $U_g$ , and  $u$  and  $v$  are the interaction displacements of the mass points of the foundation model.

### 5. Steady State Response

To examine the influence of the foundation parameters on the dynamic response of the interaction systems, five, ten and fifteen-story buildings are analyzed for both harmonic and transient excitations. These are single bay shear structures with the flexural stiffnesses taken in accordance with Housner and Brady [11] but reduced for unit length normal to the direction of vibration. The buildings have a bay width of twenty feet, equal story heights of twelve feet, floor unit weight of 100 psf and the values of  $\alpha_0$  are 1.5, 2 and 2.5 for the five, ten and fifteen-story buildings respectively. The interfloor damping coefficient  $c_n$  is taken as one percent of critical damping. In addition, the foundation medium has a unit weight of 110 pcf while Poisson's ratio and the shear wave velocity are the parameters of this study.

The differential equations of motion are solved for the harmonic excitation  $U_g = Qe^{i\omega t}$ , where  $Q$  is the amplitude. The ratio  $\theta$ , plotted versus the shear wave velocity  $V_s$  in Fig. 9, is the maximum response  $U^*$  of the interaction system divided by the corresponding maximum flexural response  $\bar{U}$  of the same building resting on a rigid foundation, i.e.,  $V_s = \infty$ . The latter case is obtained by solving the  $N$  equations given by (8c) with  $U_0 = \Psi = 0$ .



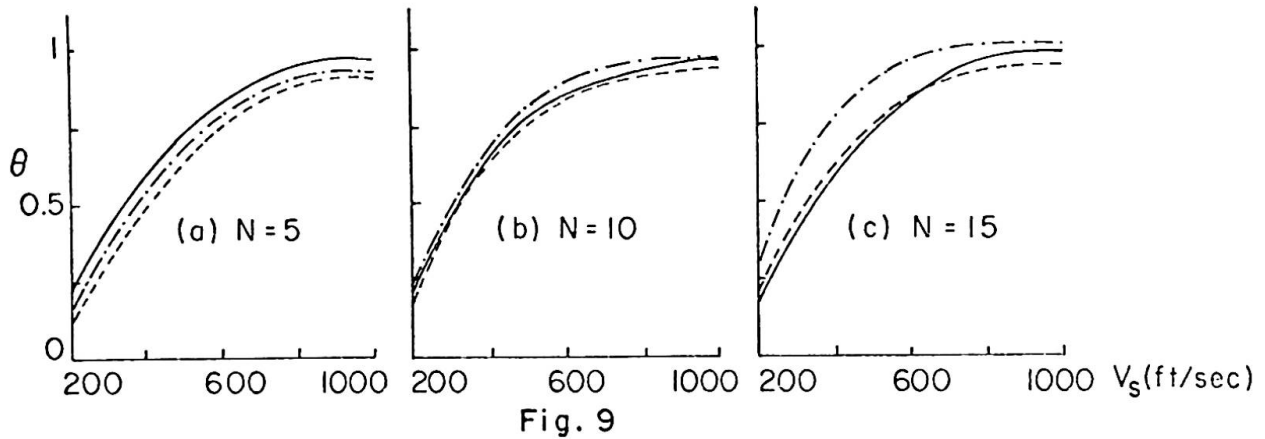


Fig. 9

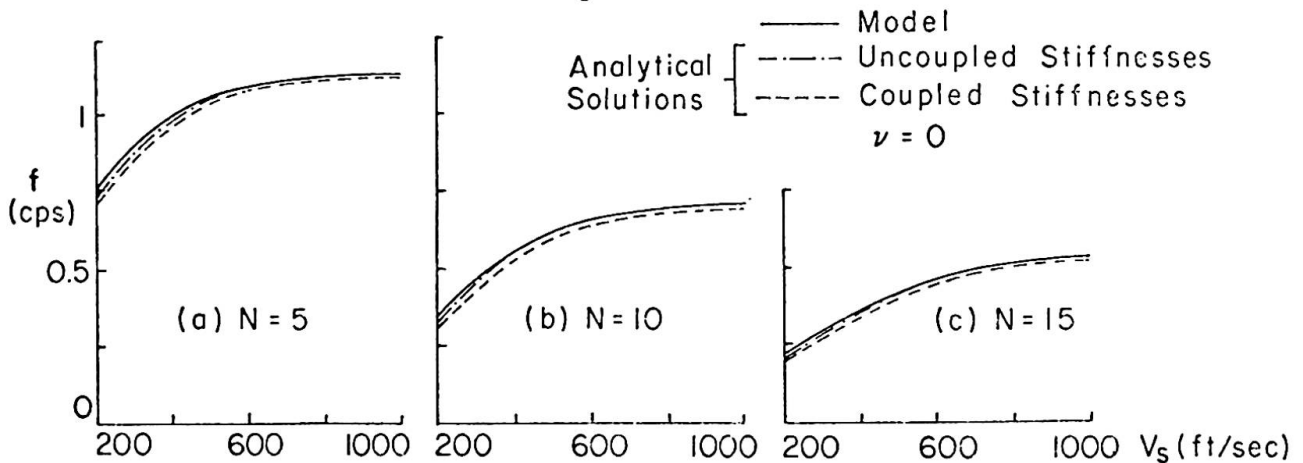


Fig. 10

Also shown in Fig. 9 are the corresponding analytical results using the stiffnesses presented by Karasudhi, Keer and Lee [10]. In their study of the harmonic rocking and horizontal vibrations of an infinitely long rectangular rigid body on an elastic half space, both uncoupled and coupled motions are considered. It was found, that while the uncoupled stiffnesses are in fairly good agreement with the diagonal elements of the stiffness matrix for the coupled vibration, the effect of the off-diagonal elements is significant. In Fig. 9 the analytical solution using the coupled stiffnesses shows consistent agreement with the results obtained from the model, while the uncoupled stiffnesses yield results which diverge from the other two solutions. Figure 10 shows the variation of the fundamental frequency  $f$  with the shear wave velocity given by the model as well as the analytical solution.

As the foundation medium becomes more flexible, i.e., as  $V_s$  decreases, the values of  $\theta$  and  $f$  decrease monotonically as shown in Figs. 9,10. For the three cases studied it is noted that foundation media with a shear wave velocity of 1000 ft/sec closely approximate the rigid foundation, and that the interaction effect is significant only for lower values.

It is evident from Figs. 9,10 that the proposed model is phenomenologically satisfactory for use in the study of the dynamic response of soil-structure interaction systems.

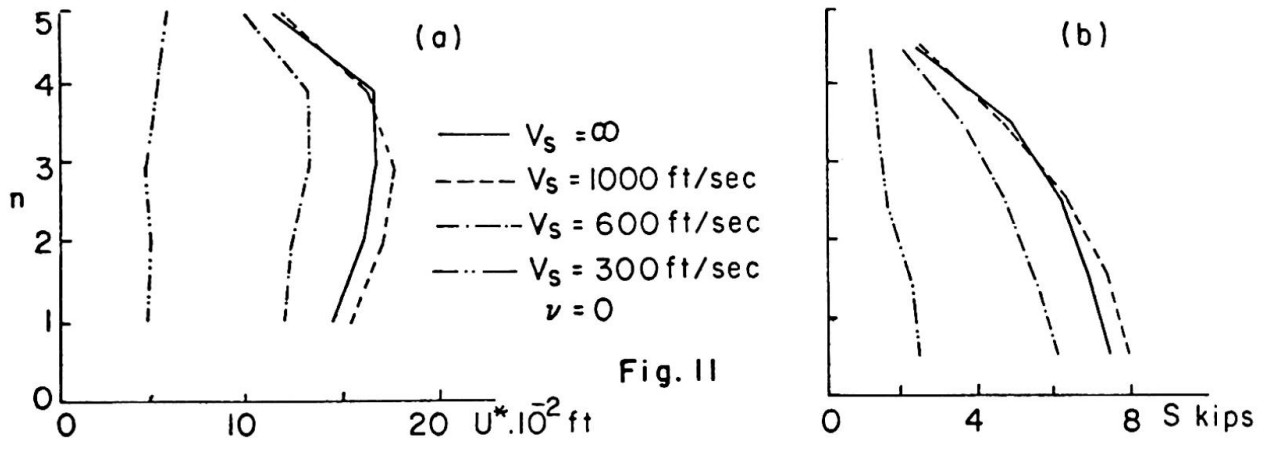


Fig. 11

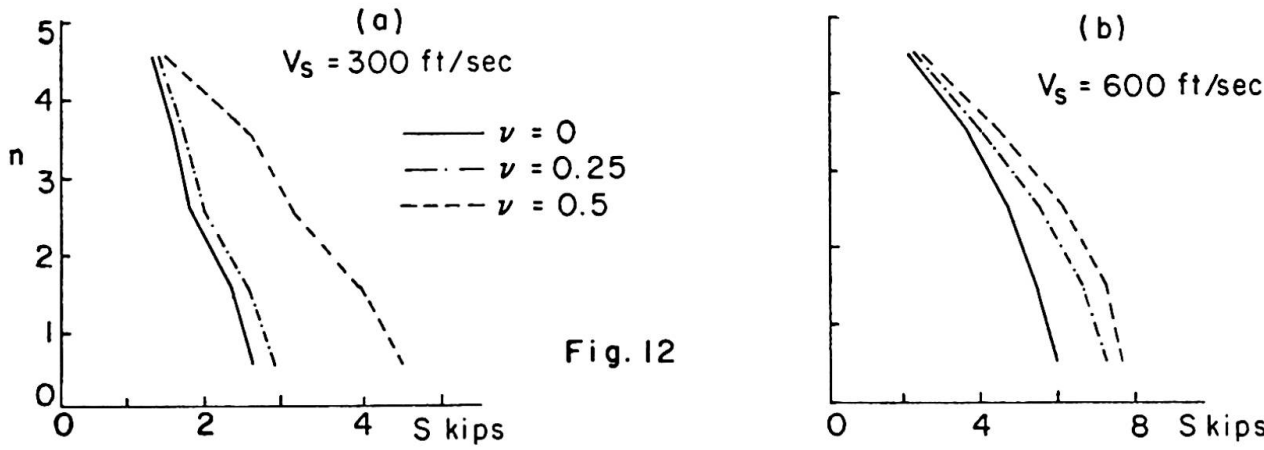


Fig. 12

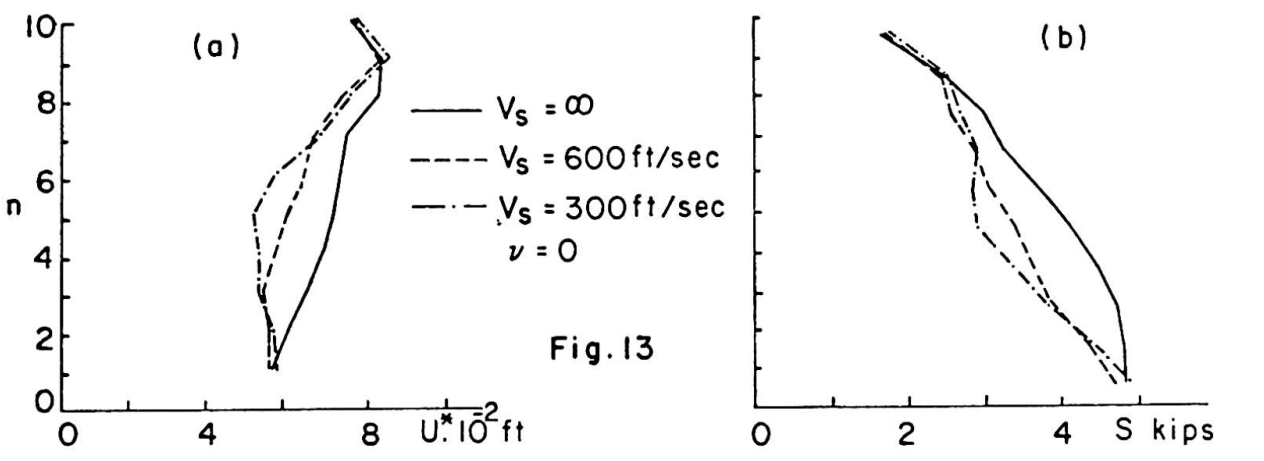


Fig. 13

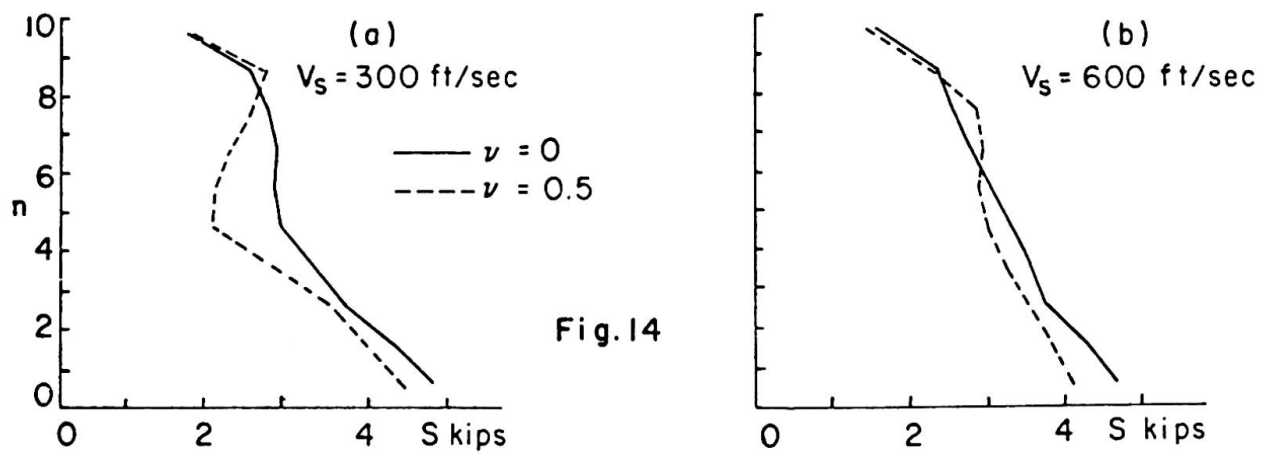


Fig. 14

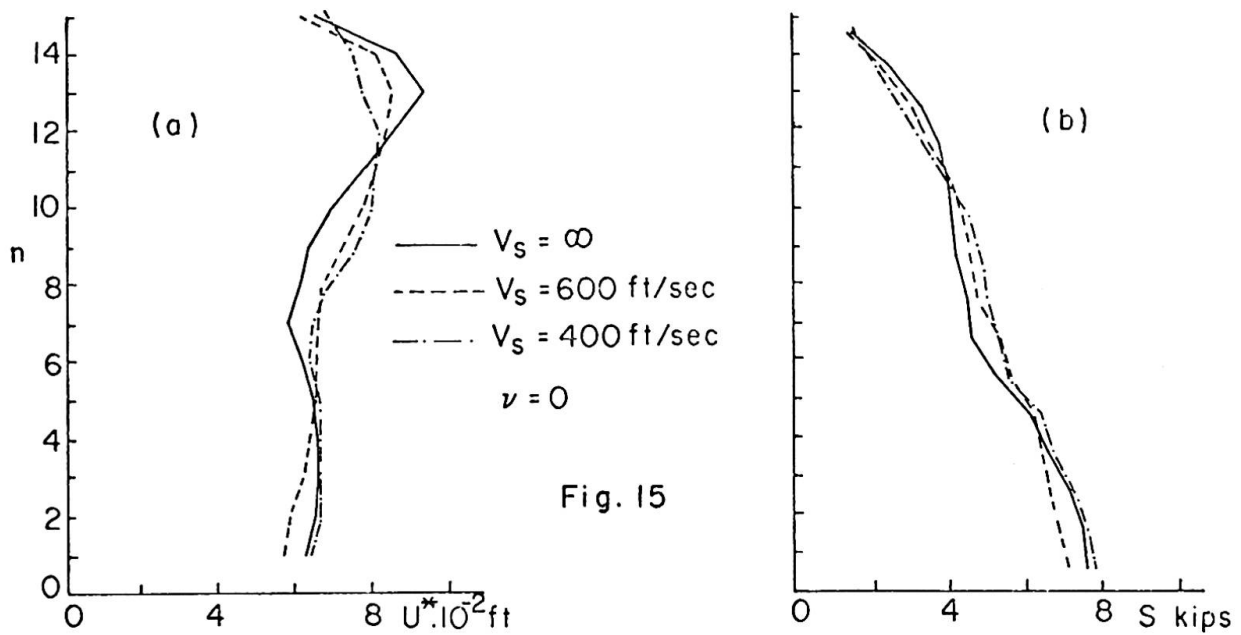


Fig. 15

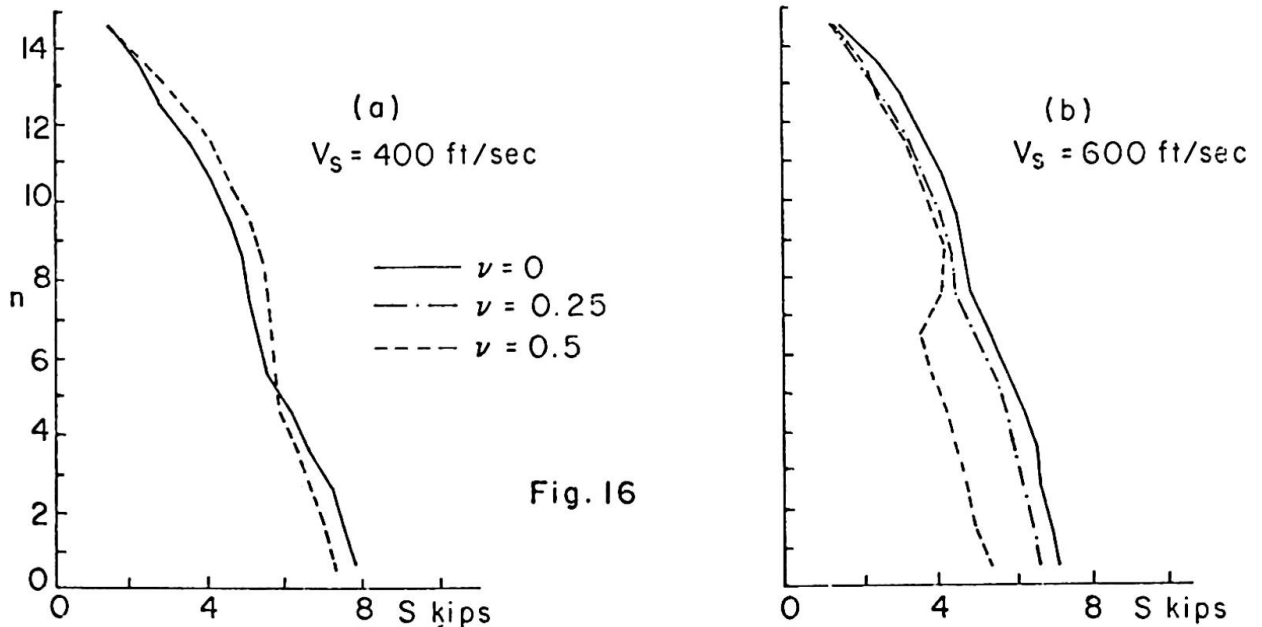


Fig. 16

### 6. Transient Response

The accelerogram for the N-S component of El Centro, California, earthquake of May 18, 1940 is used for the following investigation. The system of differential equations of motion is solved using the step-by-step numerical integration procedure suggested by Wilson and Clough [12].

Figures 11 to 16 show the effect of the foundation properties on the maximum flexural response  $U^*$  and story shears  $S$  when the three interaction systems are subjected to the above mentioned earthquake excitation in the ranges  $300 \leq V_s \leq 1000 \text{ ft/sec}$  and  $0 \leq \nu \leq 0.5$ . The corresponding results obtained for rigid foundations are also shown for comparison.

Figure 11 shows the response of the five-story building for  $\nu = 0$ . When  $V_s = 1000 \text{ ft/sec}$  the base shear is about 6% higher than the rigid case and then decreases with decreasing shear wave velocity. Unlike the ten and fifteen-story buildings, shown in Figs. 14, 16, the five-story shears increase steadily

with increasing values of Poisson's ratio as shown in Fig. 12. The high story shears are characteristic of the response of this building to the particular earthquake excitation. This type of interrelationship has been observed and discussed by many investigators [2,13]. It should be noted that the first four natural periods of the five-story building on rigid foundation coincide with as many peaks in the velocity spectrum curve for the earthquake. This fact is the major contribution to the large flexural displacements and high story shears.

The response of the ten-story building in Fig. 13 shows a general reduction in story shears with decreasing shear wave velocity and even further reduction in the lower floors (Fig. 14) as Poisson's ratio is increased from zero to 0.5. However, this pattern of behavior is not observed in the case of the fifteen-story building (Fig. 15) which shows a decrease in story shears in the lower floors for  $V_s = 600$  ft/sec, compared with the rigid case, an increase in the middle floors and again a decrease in the upper floors. On the other hand, as the shear wave velocity decreases to 400 ft/sec, an increase in story shears is observed in the lower floors and a decrease in the upper floors. The effect of increasing Poisson's ratio for  $V_s = 600$  ft/sec results in continued decrease in the story shears (Fig. 16) while for  $V_s = 400$  ft/sec the decrease is only in the lower floors followed by an increase in the upper stories.

## 7. Conclusions

A mathematically consistent lumped-parameter model of finite size to represent the elastic half plane for the study of initial and boundary-value problems is presented. The proposed model is used to investigate the effects of the flexibility of the foundation medium on the seismic response of long multi-story buildings. Damping elements are introduced along the boundaries of the model to dissipate the energy and reduce wave reflection. The model can be extended to the treatment of anisotropic and/or inelastic foundation media by incorporating the appropriate constitutive equations in the stress points.

It has been shown that the influence of the flexibility of the foundation on the seismic response of multi-story buildings is significant. The physical properties that affect the foundation stiffness and damping characteristics are the shear wave velocity and Poisson's ratio.

For steady state excitations, the flexibility of the foundation results in continued reduction in the flexural displacements, story shears and frequencies compared to the values obtained by rigid foundation. Extending these conclusions to the transient response is unjustifiable since the results for the latter show no general pattern of behavior with the variation of the foundation properties for the cases studied. The results clearly demonstrate that the effect of the flexibility of the foundation on the transient response of multi-story buildings depends not only on the characteristics and nature of the earthquake excitation, but also on the physical properties of the building as well as the foundation medium. This conclusion is in agreement with previous studies [8]. The shear wave velocity has the effect of changing the natural periods of the interaction system and thereby altering the energy input to the building indicated by the ordinates of the spectral velocity curve of the earthquake excitation.

## 8. Acknowledgements

The research upon which this paper is based was supported in part by the National Science Foundation under Grant No. GK-1910 to Northwestern University.

## 9. References

1. L. E. Goodman, E. Rosenblueth and N. M. Newmark, "Aseismic Design of Elastic Structures Founded on Firm Ground," Proc. ASCE, Vol. 79, No. 349, Nov. 1953.
2. R. W. Clough, "Dynamic Effects of Earthquakes," Trans. ASCE, Vol. 126, Part 2, 1961, pp. 847-876.

3. K. Suyehiro, "Engineering Seismology, Notes on American Lectures," Proc. ASCE, Vol. 58, No. 4, Part 2, May 1932.
4. R. Tanabashi and H. Ishizaki, "Earthquake Damages and Elastic Properties of the Ground," Bulletin Disaster Prevention Research Inst., Kyoto Univ., No. 4, May 1953.
5. R. G. Merritt and G. W. Housner, "Effect of Foundation Compliance on Earthquake Stresses in Multistory Buildings," Bulletin of the Seismological Society of America, Vol. 44, No. 4, Oct. 1954, pp. 551-569.
6. D. L. Lycan and N. M. Newmark, "Effect of Structure and Foundation Interaction," Proc. ASCE, Journal Eng. Mech. Div., Vol. 87, No. EM5, Oct. 1961, pp. 1-31.
7. R. A. Parmelee, "Building-Foundation Interaction Effects," Proc. ASCE, Journal Eng. Mech. Div., Vol. 93, No. EM2, April 1967, pp. 131-152.
8. R. A. Parmelee, D. S. Perelman and S. L. Lee, "Seismic Response of Multiple-Story Structures on Flexible Foundations," submitted for publication.
9. A. H.-S. Ang and G. N. Harper, "Analysis of Contained Plastic Flow in Plane Solids," Proc. ASCE, Journal Eng. Mech. Div., Vol. 90, No. EM5, Oct. 1964, pp. 397-418.
10. P. Karasudhi, L. M. Keer and S. L. Lee, "Vibratory Motion of a Body on an Elastic Half Plane," submitted for publication.
11. G. W. Housner and A. G. Brady, "Natural Periods of Vibration of Buildings," Proc. ASCE, Journal Eng. Mech. Div., Vol. 89, No. EM4, Aug. 1963, pp. 31-65.
12. E. L. Wilson and R. W. Clough, "Dynamic Response by Step-by-Step Matrix Analysis," Symposium on the Use of Computers in Civil Engineering, Paper No. 45, Lisbon, Portugal, Oct. 1962.
13. G. W. Housner, "Behavior of Structures During Earthquakes," Proc. ASCE, Vol. 85, No. EM4, Oct. 1959, pp. 109-129.

## SUMMARY

## Summary

A mathematically consistent lumped-parameter model of finite size to simulate the elastic half space for investigating the effects of the flexibility of the foundation on the seismic response of long multi-story buildings is presented. Appropriate damping elements are introduced at the boundaries to dissipate energy and reduce wave deflection. The proposed model yields phenomenologically satisfactory results as evidenced by a comparison with the results obtained by analytical solutions for the steady state response of several soil-structure interaction systems.

A parametric study of the transient response of soil-structure systems shows that the foundation flexibility modifies the response of the structure in comparison with rigid foundation and that the effects depend on the physical properties of the structure and the foundation medium, as well as the characteristics of the earthquake excitation.

## RÉSUMÉ

Cette contribution présente un modèle de grandeur finie, mathématiquement valable, avec paramètres adéquats, simulant le demi-espace élastique. Ce modèle permet l'étude de la flexibilité des fondations sous des secousses sismiques sur des constructions longues à beaucoup d'étages. Des amortisseurs appropriés ont été utilisés sur les bords pour dissiper l'énergie et pour réduire la déflexion des ondes. Le modèle proposé donne des résultats phénoménologiquement satisfaisants, comme le démontre la comparaison avec les calculs analytiques sur plusieurs systèmes.

Une étude paramétrique montre que la réaction de la construction dépend de la flexibilité des fondations, et que les effets dépendent des propriétés physiques de la structure et des fondations aussi bien que des caractéristiques de l'excitation sismique.

## ZUSAMMENFASSUNG

Ein mathematisch verträgliches Modell endlicher Grösse mit "Umfassungs"-Parameter zur Nachahmung des elastischen Halbraums für Untersuchungen der Fundamentsteifigkeit unter Erdbeben wird für lange mehrstöckige Bauten angegeben. Es sind an den Rändern Dämpfungselemente eingeführt worden, um die Energie zu verbrauchen sowie die Wellenausschläge zu vermindern. Das vorgeschlagene Modell ergibt phänomenologisch befriedigende Ergebnisse im Vergleich mit denjenigen der analytischen Lösung.

Eine Parameter-Studie der Uebergangsbestimmung der Bodenstrukturen zeitigt, dass die Fundamentsteifigkeit die Bestimmung der Struktur im Vergleich mit steifen Fundamenten verändert, und dass die Wirkung von den physikalischen Verhältnissen der Struktur, des Fundamentes und sowohl als auch von der Erdbebencharakteristik abhängt.

Leere Seite  
Blank page  
Page vide